



HAL
open science

Small gold nanoparticles for tandem cyclization/reduction and cyclization/hydroalkoxylation reactions

Kristína Plevová, Véronique Michelet, Sylvain Antoniotti

► **To cite this version:**

Kristína Plevová, Véronique Michelet, Sylvain Antoniotti. Small gold nanoparticles for tandem cyclization/reduction and cyclization/hydroalkoxylation reactions. *Communications Chemistry*, 2024, 7 (1), pp.248. 10.1038/s42004-024-01336-7 . hal-04760817

HAL Id: hal-04760817

<https://hal.science/hal-04760817v1>

Submitted on 30 Oct 2024

HAL is a multi-disciplinary open access archive for the deposit and dissemination of scientific research documents, whether they are published or not. The documents may come from teaching and research institutions in France or abroad, or from public or private research centers.

L'archive ouverte pluridisciplinaire **HAL**, est destinée au dépôt et à la diffusion de documents scientifiques de niveau recherche, publiés ou non, émanant des établissements d'enseignement et de recherche français ou étrangers, des laboratoires publics ou privés.



Distributed under a Creative Commons Attribution - NonCommercial - NoDerivatives 4.0 International License

<https://doi.org/10.1038/s42004-024-01336-7>

Small gold nanoparticles for tandem cyclization/reduction and cyclization/hydroalkoxylation reactions

Check for updates

Kristína Plevová, Véronique Michelet & Sylvain Antoniotti

With peculiar structural features at the surface of small metal nanoparticles, some discrete sites can display catalytic behaviour similar to what could be observed with mononuclear metal catalysts in solution. We have studied the transfer of two catalytic tandem reactions from homogeneous to heterogeneous conditions. Tandem cyclisation/reduction of *ortho*-alkynyl benzaldehyde derivatives was successfully achieved with Au nanoparticles over TiO₂ (Au NPs/TiO₂) in the presence of Hantzsch ester with 45–98% yields for 15 examples (average yield: 70.4%). Similarly, tandem cyclisation/hydroalkoxylation of *ortho*-alkynyl benzaldehyde derivatives was successfully achieved with Au NPs/TiO₂ in methanol or other alcohols with 62–96% yields for 17 examples (average yield: 84.9%). The application potential of this catalytic system was demonstrated with the total synthesis of a bioactive isochromene derivative featuring one of the developed reactions as the key step and the implementation of the tandem cyclisation/hydroalkoxylation in a continuous flow reactor, scaling up the reaction by a factor of 10 without loss of efficiency.

Although early reports on the use of gold in catalysis by Hutchings and Haruta described both the use of gold nanoparticles and gold salts^{1–3}, the rush observed in the last decades has massively focused on homogeneous gold catalysis^{4–9}. Heterogeneous gold catalysis, either by heterogenization of gold complexes through immobilisation techniques or by using gold nanoparticles as catalysts^{10–13}, has begun to receive renewed attention more recently.

A major objective of transferring a reaction from homogeneous to heterogeneous protocols is the associated practical advantages such as facilitated recycling of the catalysts and easier implementation in continuous flow with fixed-bed catalytic reactors¹⁴. Beyond the higher surface-to-volume ratios and some physicochemical features of the supports (typically MO_x like TiO₂, Al₂O₃, ZnO for inorganic supports) that influence reaction mechanisms (e.g., Brønsted or Lewis acidity, formation of intermediates covalently bound to the support, or redox reactions), it is increasingly documented that small nanoparticles exhibit particular features at their surface such as steps, edges and corners where catalysis is taking place^{15–18}. Metal nanoparticles with controlled shapes, such as crystal structures and planes, can now be produced reliably with low dispersity¹⁹. The same applies to bimetallic nanoparticles existing either as alloy, core-shell, near surface alloy or doped metal objects²⁰.

More specifically in the case of Au NPs, singularised atoms such as adatoms (adsorbed atoms), although considered at the 0 oxidation state, can behave as cationic species by delocalisation of electrons within the particle,

and although without bearing a formal charge have a catalytic activity similar to that of homogeneous mononuclear gold complexes^{21–23}. At even lower sizes, gold nanoclusters consisting of 3–10 atoms were reported to be highly active in the hydration of alkynes with a turnover number of 10^{–7}^{17,24}. This finding revealed the most intimate missing link between homogeneous and heterogeneous gold catalysis, although many chemists familiar with the use of gold salts in catalysis had already noticed the purple colouring of the reaction mixture suggesting the formation of such nanoclusters/nanoparticles.

In the early 2010s, the use of commercial nanoparticles in relatively sophisticated reactions appeared in the literature^{25,26}, although at that time knowledge of the connection to structural features at the nanoparticle surface and ideas of adatoms were not widespread. Au NPs with a size below 3 nm have been successfully used in cycloisomerisation of 1,6-enynes²⁷, and even involved in a cascade Diels–Alder reaction²⁸. In the latter example, the surface was functionalized with bulky thiols ligands and intentionally oxidised to provide formal cationic gold species at the surface, stabilised by ditopic polymantane sulfonate anions that also prevent these very small nanoparticles from aggregating.

There is still a gap, however, between homogeneous and heterogeneous catalysis, and transfer from the former to the latter is generally achieved at the expense of yields, energy demand, substrate scope or applicability. We have been working in our laboratory on gold catalysis either under homogeneous conditions^{29–32} or under heterogeneous conditions using supported gold nanoparticles in tandem or sequential one-pot schemes that exploit

small nanoparticles^{33–35} or larger ones³⁶, which behave more as stabilising surfaces for intermediates than actual catalysts, lowering the energy barrier to reach a given transition state. In the present paper, we describe our results of tandem reactions at the surface of small Au NPs (<3 nm), inspired by Au-catalysed processes such as the cyclisation/reduction³⁷ and Pd-catalysed cyclisation/hydroalkoxylation³⁸ of *ortho*-alkynyl benzaldehyde derivatives. These approaches were then successfully applied to a short total synthesis of an isochromene derivative of biological interest. The methods developed were also implemented in a continuous flow reactor to demonstrate their potential for scaling up.

Considering the recent progress in the understanding of the catalytic activity of small nanoparticles and inspired by previous work reported by one of us, we first investigated the possibility of activating *ortho*-alkynyl benzaldehyde substrates to trigger a cyclisation/reduction sequence and access valuable 1H-isochromene derivatives³⁷. We had in hand Au NPs on various supports and performed TEM analysis to check the shape, size and dispersity (see Supplementary Information, SI).

Results and discussion

In order to find the optimal reaction conditions for the cyclisation/reduction sequence, 2-(phenylethynyl)benzaldehyde (**1a**) was selected as a model substrate and Hantzsch ester (HEH) was used as the reducing agent (Table 1, for more details on the optimisation see SI). The screening of conditions started with small gold nanoparticles (Au NPs) supported on different types of inorganic oxides such as TiO₂, Al₂O₃ or ZnO (Table 1, entries 1–3). Larger Au NPs were also tested but gave poor or no results (see SI). The best result in terms of selectivity, conversion and yield was obtained when Au NPs/TiO₂ was used as a catalyst (Table 1, entry 3). It is worth mentioning that, even though the reaction could lead to the formation of 6-*endo* or 5-*exo* cyclisation products, our reaction under these conditions was found to be exclusively 6-*endo* selective. To increase the reaction yield, screening of other solvents was performed (Table 1, entries 4–7). The best result remained that with toluene at 80 °C (Table 1, entry 3). An interesting result was obtained with MeOH as the solvent, with the formation of a mixture of two products—reduction product **2a** and hydroalkoxylation product **3a** (Table 1, entry 7).

The desired 1H-isochromene **2a** was thus obtained as the single product, the reaction thereby proceeding with 100% 6-*endo* selectivity, with 100% conversion and 69% yield after isolation. This result prompted us to prepare a library of suitable substrates **1a–o** by using Sonogashira cross-coupling starting from the corresponding commercially available *ortho*-bromobenzaldehyde derivatives with variations both at the benzaldehyde motif and the aryl substituent (see SI). These substrates reacted smoothly under our optimised conditions to deliver the expected products **2a–o** in 45–98% yield (Fig. 1). The desired 1H-isochromene derivatives **2a–o** were obtained as a single product, the reaction thereby proceeding again with 100% 6-*endo* selectivity.

Electronic effects of substituents R¹ on benzaldehyde as well as R² on the aryl moiety influenced the electrophilicity of both alkyne carbon atoms. The presence of electron-donating groups on the benzaldehyde moiety (Fig. 1, products **2b**, **2d**, **2e**) increased the electronegativity of both the aldehydic carbonyl function and the alkyne, thus favouring the reaction. Substitution of the aryl moiety with electron-withdrawing groups (Fig. 1, product **2j**) should increase the electrophilicity of the vicinal alkyne carbon atom and thus favour a 5-*exo* attack³⁹. On the contrary, the reaction led again to the exclusive formation of the 6-*endo* product **2j**, albeit in lower yield (55%). In the case of aliphatic substituents attached directly to alkyne, full conversion of substrates was achieved after 1 h, but products **2n** and **2o** were isolated in 45% and 57% yield, respectively. Lower yields could be explained by the instability of these substrates under the relatively high temperature (80 °C) that is crucial for this transformation to be successful (for optimisation, see SI). Introduction of a pyridine motif, of -NO₂ or -CN substituents at the para position of the aryl moiety was detrimental to the reaction, presumably due to the formation of complexes between Au NPs and nitrogen atoms (not shown, see SI)³⁹.

Negative controls confirmed the catalytic role of Au NPs, and inductively coupled plasma optical emission spectroscopy (ICP-OES) titration of residual homogeneous gold species in the reaction mixture was found to be 0.3 ppm, thereby ruling out the hypothesis of hidden homogeneous catalysis by erosion of the Au NP surface (see SI). Observations of fresh and used Au NPs/TiO₂ samples by STEM-HAADF-BF did not identify any differences between the two, suggesting the catalytic material was unchanged at the nanometric scale (see SI). Activation of the triple bond of our substrates at the Au NP surface to allow for the nucleophilic attack of the carbonyl function was thus effective. Encouraged by this result observed during optimisation (Table 1, entry 7), we decided to further exploit this reactivity by introducing MeOH as the nucleophile instead of HEH to potentially catalyse a cyclisation/hydroalkoxylation sequence (Fig. 2).

Similar reactivity was described under homogeneous conditions with Pd(OAc)₂³⁸, AgSbF₆⁴⁰ or CuI^{41,42} as the catalyst. Interestingly, Belmont's work⁴⁰ also described the very poor activity of Au as the catalyst for this sequence. In the context of all published results, we were very pleased to observe that under our optimised conditions using Au NPs/TiO₂ and MeOH as nucleophile and solvent, the reaction proceeded smoothly, and the corresponding ketals **3a–o** were isolated in excellent yields (Fig. 3).

The reaction tolerated electron-donating groups very well and delivered the products **3a–o** in an exclusively 6-*endo* selective manner. In some cases, full conversion of the starting material in MeOH was not achieved, even after prolonged reaction times (for more details see SI). In these cases, a lower solubility of the substrate in MeOH was observed, so the reaction protocol was modified (Fig. 2, products **3e–h**, **3j**, **3k**). Different combinations of solvents were tested, and the best result was obtained when a mixture of DMF/MeOH (1:1) was used. We note that the reaction, using both protocols, did not require any additional purification.


If methanol was replaced by another alcohol such as ethanol, *iso*-propanol or cyclohexanol, the reaction led to the formation of the expected 6-*endo* products **4a–6a** in moderate to excellent yields (Fig. 4). In the case of secondary alcohols, slightly longer reaction times were required to achieve full conversion. To enlarge the scope, we also tested the secondary alcohol as the reagent. Different loads of cyclohexanol (1.2, 4 and 5 equiv.) in DMF were tested, but unfortunately, after 4 h only traces of product were observed. If the reaction time was extended overnight, only the decomposition of the starting material **1a** was observed.

In contrast with the previous reaction using HEH, which is poorly soluble in toluene, using MeOH as both the solvent and the nucleophile resulted in a particularly simple protocol. The reaction could thus easily be transferred to a continuous flow reactor. A fixed-bed catalytic column was assembled with 5 g of Au NPs/TiO₂. In the optimised conditions (see SI for optimisation), a residence time of 3.3 min was observed at the steady state and 2 g of product **3a** was easily isolated in 87% yield (Table 2). The reaction was thus found to be linearly scalable by a factor of 10, and the target product **3a** was obtained in higher yields than in batch reactions.

The isochromene motif is frequently observed in natural products sometimes showing interesting biological properties such as antibacterial, antifungal, antitumoral or antimicrobial activity (Fig. 5).

The most popular method to access the isochromene motif, from the perspective of atom economy, is the use of transition metal-catalysed cyclisation of *ortho*-alkynylarylaldehydes or *ortho*-alkynylbenzylalcohols. The heterogeneous catalysis we have developed could be an attractive alternative to this homogeneous catalysis.

The optimised reaction conditions were thus applied as a key step in total synthesis of methyl 1,5,8-trimethoxy-1H-isochromene-3-carboxylate **10**—a known compound for antitumor activity against breast cancer (Fig. 6)⁴³. First, protection of aldehyde **7** was performed, which led to the formation of the corresponding acetal, then *ortho*-lithiation was followed by reaction with 1,2-diiodoethane to give the 2-iodo-3,6-dimethoxybenzaldehyde **8** in 33% yield over three steps. Halogenated benzaldehyde **8** was then used in the Sonogashira coupling reaction with TMS-acetylene, followed by TMS removal to give the terminal alkyne. Deprotonation of this alkyne with *n*BuLi was firstly performed with unprotected aldehyde as

Table 1 | Optimisation of reaction conditions for the cyclisation/reduction sequence of **1a catalysed by Au NPs/TiO₂ in the presence of Hantzsch ester.^[a]**


Entry	[Au NPs]	Solvent	Temp.	Conv. ^[b] (Yield %) ^[c]	6-endo/5-exo 2a:2a'
1	Au/Al ₂ O ₃	toluene	80 °C	24%	86:14
2	Au/ZnO	toluene	80 °C	29%	92:8
3	Au/TiO ₂	toluene	80 °C	100% (69%) ^[c]	>99:0
4	Au/TiO ₂	toluene	70 °C	60%	>99:0
5	Au/TiO ₂	CH ₃ CN	70 °C	11%	>99:0
6	Au/TiO ₂	THF	70 °C	16%	>99:0
7	Au/TiO ₂	CH ₃ OH	70 °C	43% ^[d]	>99:0

^[a]Reaction conditions: substrate **1a** (5 mmol), [Au] (2.5 mol%), solvent (dry, 0.25 M), nitrogen atmosphere, 80 °C, 2 h.^[b]Determined by ¹H NMR.^[c]Isolated yields.^[d]Reduction product **2a**/hydroalkoxylation product **3a** = 77:23.

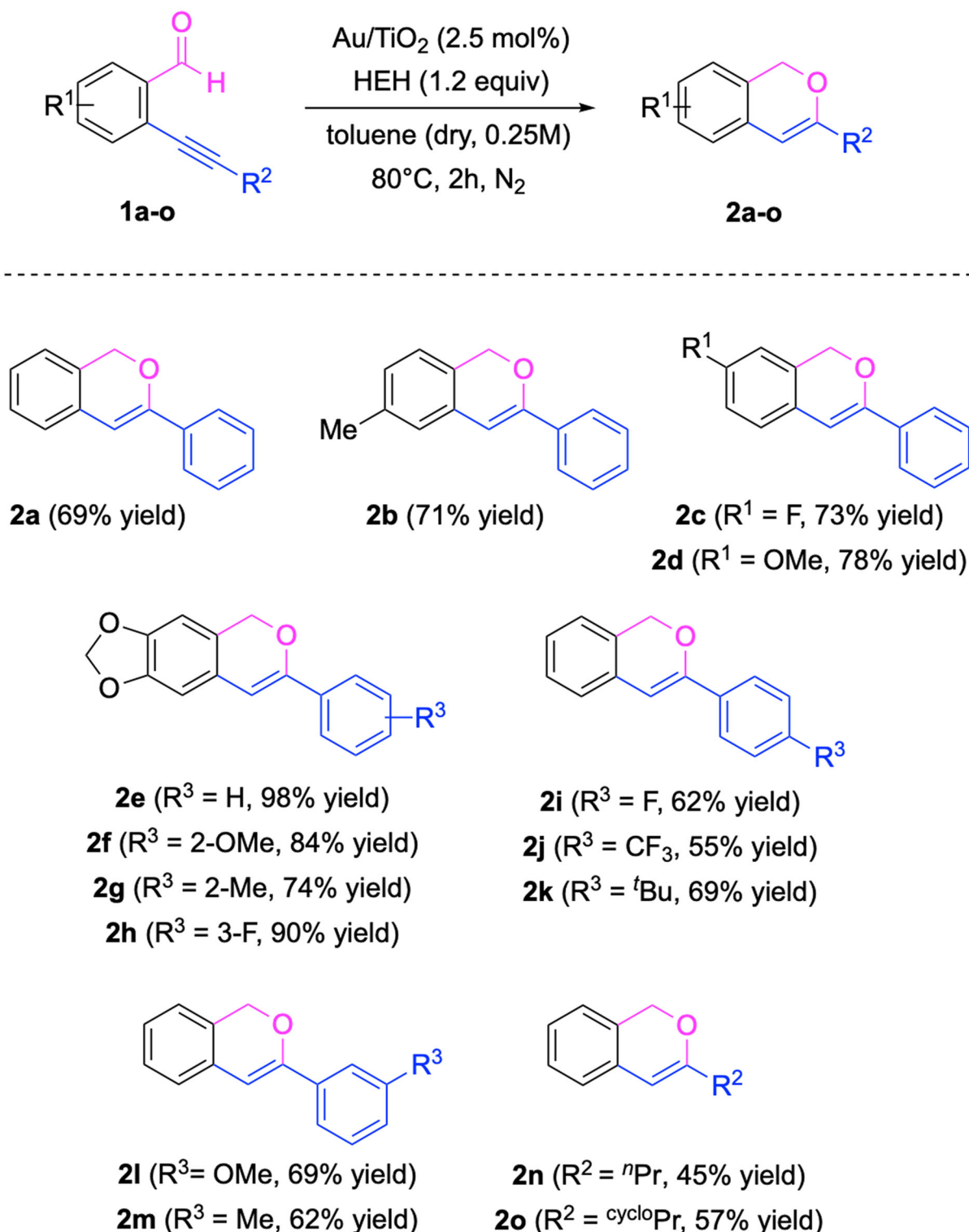


Fig. 1 | Scope of the reaction with variations of R^1 , R^2 and R^3 substituents. Au NPs/ TiO_2 -catalysed cyclisation/reduction of *ortho*-alkynyl benzaldehyde derivatives in the presence of HEH.

previously reported but unfortunately in our hands, the reaction did not lead to the desired product. Thus, protection of the aldehyde by acetalization had to be incorporated into the reaction scheme. Acetal was then subjected to deprotonation of the terminal alkyne with $n\text{BuLi}$, followed by reaction with methyl chloroformate proceeding smoothly to the target propiolate **9** in 11% yield over five steps. The last step in our total synthesis was the tandem cyclisation/hydroalkoxylation reaction catalysed by Au NPs supported on TiO_2 . After 3 h, full conversion of starting material **9** was observed and the

reaction led to formation of target product **10** in 75% yield. In contrast to the previous results, the reaction was not exclusively 6-*endo* selective, 6-*endo* and 5-*exo* cyclisation products being formed in the ratio 2:1.

Taking advantage of the peculiar morphology and properties of small gold nanoparticles (<3 nm), we have successfully transferred two tandem reactions from homogeneous to heterogeneous conditions. Tandem cyclisation/reduction of *ortho*-alkynyl benzaldehyde derivatives was achieved with Au NPs/ TiO_2 in the presence of Hantzsch ester with 45–98% yields in

Fig. 2 | An optimised isolated yield of 74% was observed. Optimised conditions for the cyclisation/hydroalkoxylation sequence of **1a** catalysed by Au/TiO₂ in methanol.

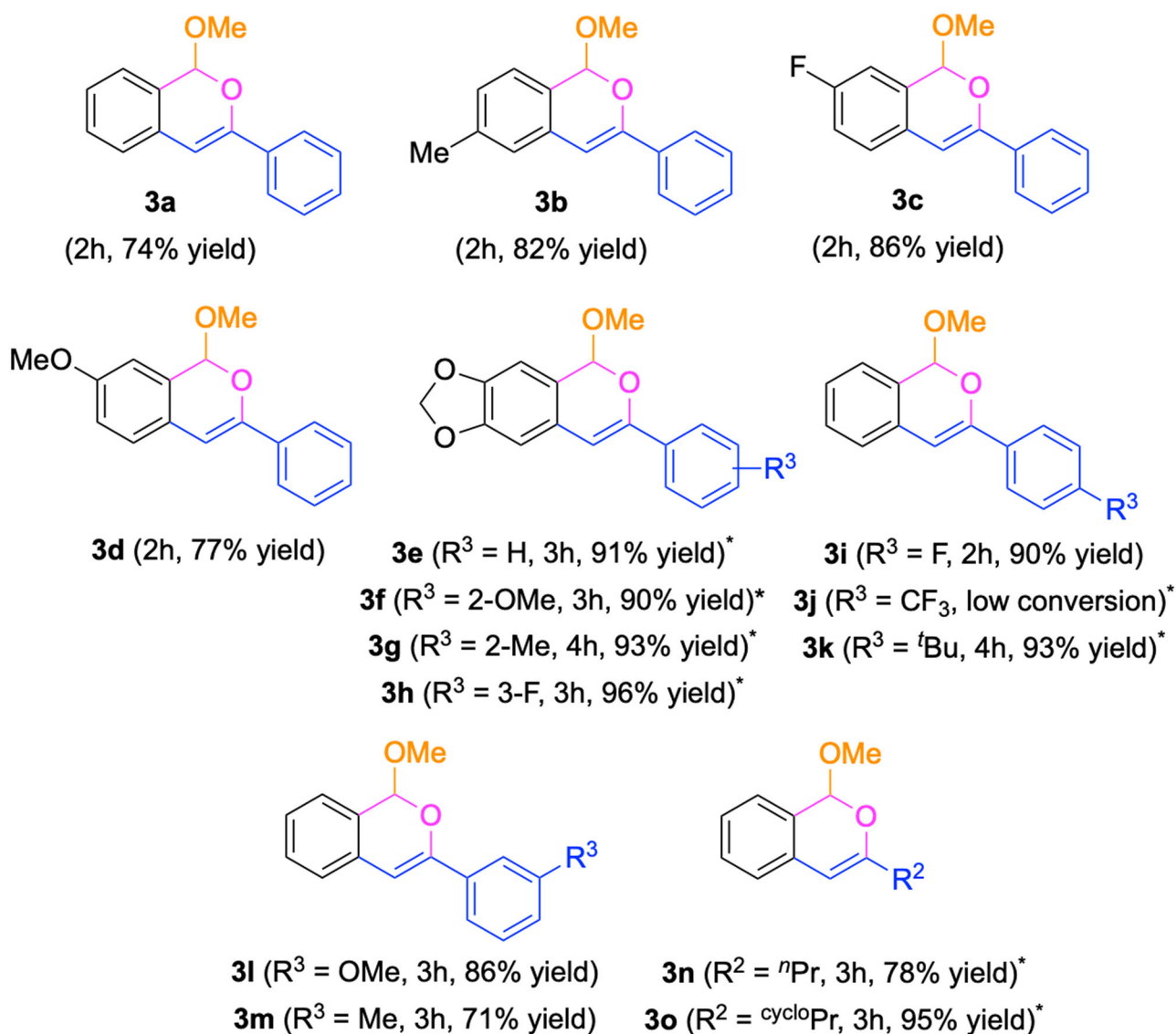
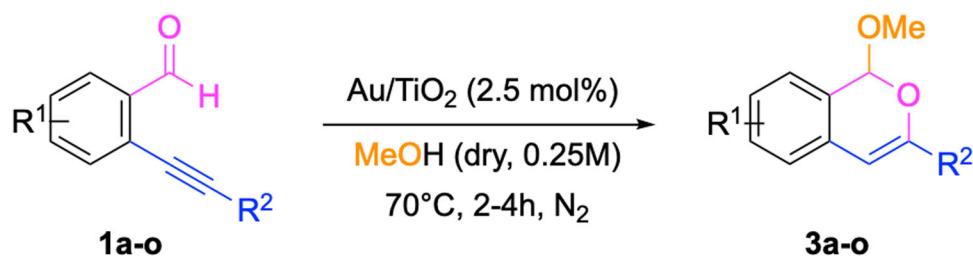
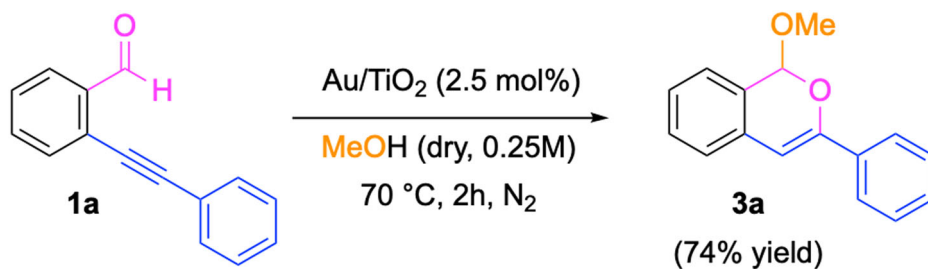


Fig. 3 | Au NPs/TiO₂-catalysed cyclisation/hydroalkoxylation of *ortho*-alkynyl benzaldehyde derivatives in MeOH. * A mixture of DMF/MeOH = 1:1 was used as a solvent.

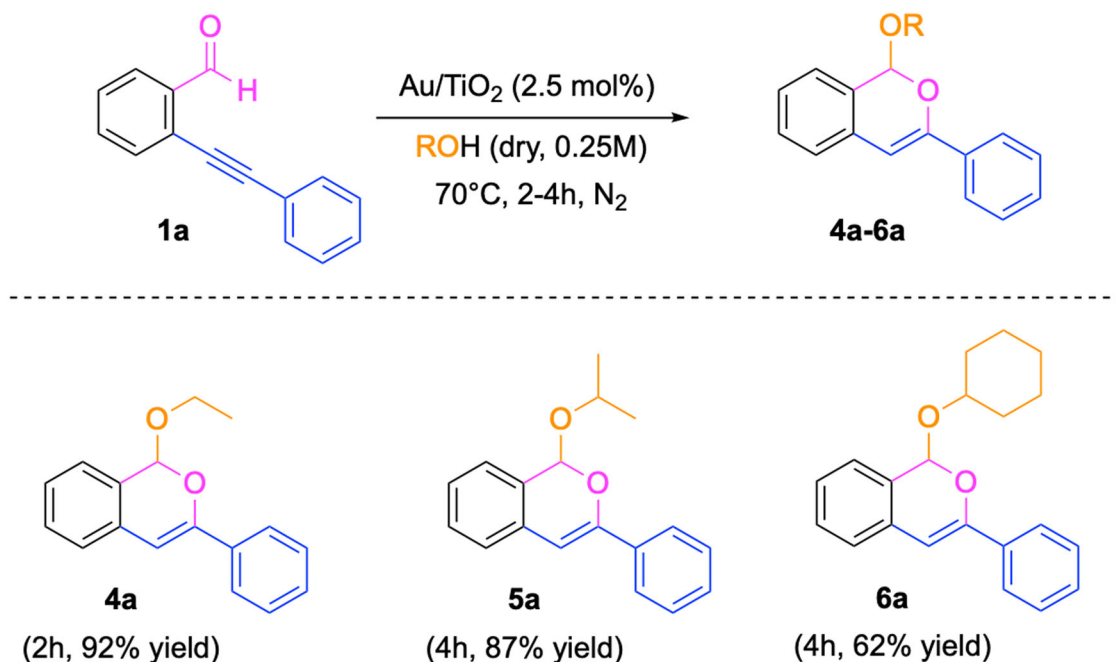


Fig. 4 | Examples of primary and secondary alcohols used as both the solvent and nucleophile are presented. Au NPs/TiO₂-catalysed cyclisation/hydroalkoxylation of *ortho*-alkynyl benzaldehyde derivatives with various alcohols as nucleophiles.

Table 2 | Cyclisation/hydroalkoxylation of **1a** catalysed by Au/TiO₂ in methanol in a continuous flow reactor

Entry	1a	Yield	6-endo/5-exo 3a:3a'
1 ^[a]	1 mmol	77%	>99:0
2	1 mmol	83%	>99:0
3	2 mmol	86%	>99:0
4	9.7 mmol	87%	>99:0

^[a]Flow: 2 mL/min.

15 examples (average yield: 70.4%). Tandem cyclisation/hydroalkoxylation of *ortho*-alkynyl benzaldehyde derivatives was achieved with Au NPs/TiO₂ in methanol and other alcohols with 62–96% yields in 17 examples (average yield: 84.9%). Besides its efficiency and sustainable profile (atom economy, waste prevention, safety), the practical potential of this catalytic system was demonstrated through the total synthesis of a bioactive isochromene featuring one of the developed reactions as the key step and the implementation of tandem cyclisation/hydroalkoxylation in a continuous flow reactor, scaling up the reaction by a factor of 10 without loss of efficiency. The development of such approaches could be of great interest in the future for applications of homogeneous gold catalysis which bring valuable fundamental knowledge but rarely find practical application. Homogeneous gold catalysis would thus remain a powerful discovery tool, while heterogeneous catalysis with small gold nanoparticles could be incorporated into sustainable processes for applications.

Methods

All solvents and reagents are commercially available from Sigma Aldrich or TCI and were used without additional purification unless otherwise mentioned.

Reactions were carried under inert atmosphere using balloon filed with N₂. Reactions were monitored by thin-layer chromatography (TLC) carried out on silica plates, visualised by irradiation with UV light in combination with *p*-anisaldehyde or KMnO₄ solution. The solution of *p*-anisaldehyde have been prepared with 135 mL of absolute ethanol, 5 mL of concentrated sulfuric acid, 1.5 mL of glacial acetic acid and 3.7 mL of *p*-anisaldehyde vigorously stirred and stored in a jar covered with an aluminium foil.

Purifications of products have been performed over silica gel (Sigma-Aldrich, pore size 60Å, 230-400 mesh particle size, 40–63 μm particle size), or alumina (Sigma-Aldrich, activated, neutral, Brockmann Activity I).

¹H and ¹³C NMR spectra were recorded on Bruker AV400 spectrometer system 400 (400 MHz for ¹H nuclei and 100 MHz for ¹³C nuclei). Chemical shifts are reported in δ units using parts per million (ppm). Signals are referenced to TMS as an internal standard. Coupling constants (*J*) are given in Hz and multiplicity is abbreviated as follows: s=singlet, d=doublet, t=triplet, q=quadruplet, quint=quintuplet, hex=t=hexuplet, hept=heptuplet and m=multiplet.

Gas chromatography coupled with Mass Spectrometry (GC-MS) was performed on Agilent model 7820 A and MS5977B using SAPIENS-5MS

Fig. 5 | These examples show the diversity and interest of isochromene derivatives as bioactive molecules. Naturally occurring bioactive isochromene compounds.

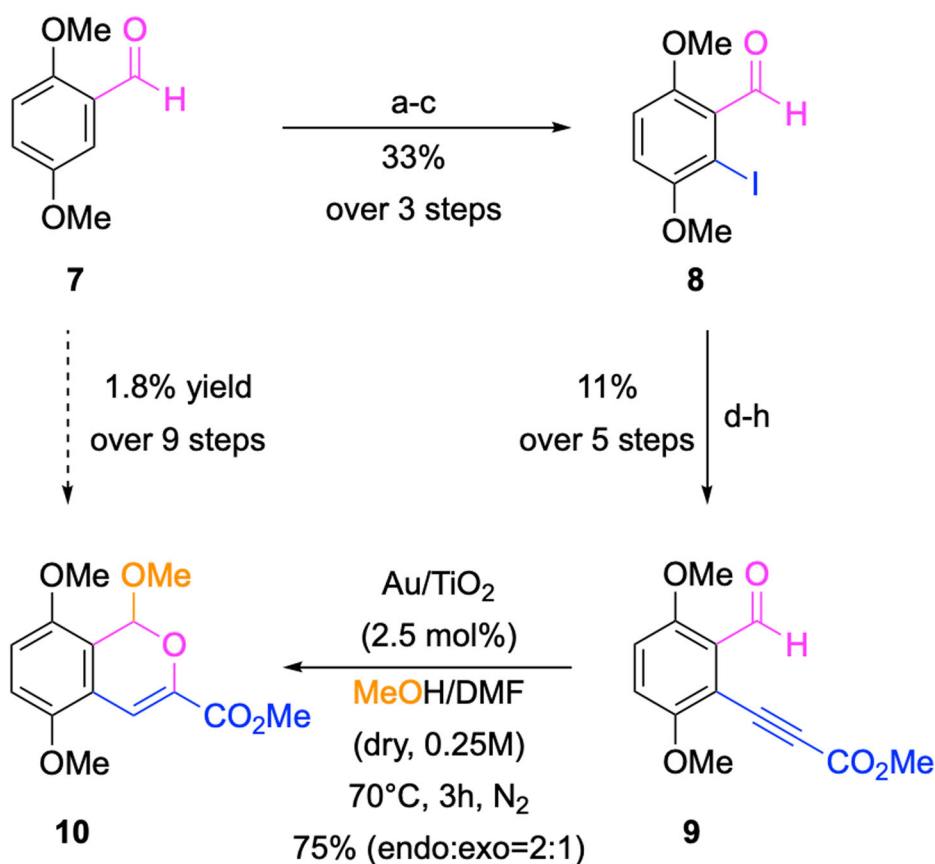
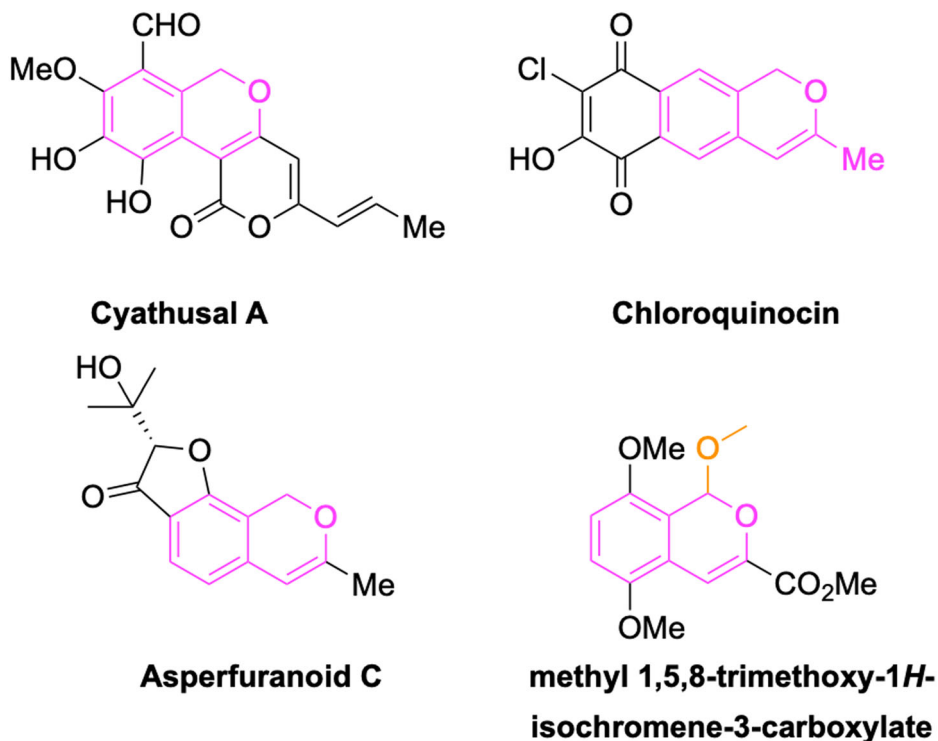


Fig. 6 | Total synthesis of 10 with the cyclisation/hydroalkoxylation sequence as the key step. Reagents and conditions: a) 1,3-propanediol (4 equiv.), (MeO)₃CH (1.1 equiv.), TBATB (1 mol%), rt, 3 h; b) ^tBuLi (1.5 equiv., 2.5 M in hexanes), benzene/hexane (1:3, 0.1 M, dry), -10 °C, 2 h; then 1,2-diiodoethane (2 equiv.), THF (1 M, dry), -10 °C-rt, overnight; c) 36% HCl (60 equiv.), THF (0.18 M), 0 °C-rt, 4 h; d) trimethylsilylacetylene (1.2 equiv.), Pd(PPh₃)₂ (2.5 mol%), CuI (1.5 mol%), toluene/

Et₃N = 3:1 (0.2 M, dry), rt, overnight; e) K₂CO₃ (10 mol%), MeOH (0.25 M, dry), rt, 2 h; f) 1,3-propanediol (4 equiv.), (MeO)₃CH (1.1 equiv.), TBATB (1 mol%), rt, 3 h; g) ^tBuLi (3 equiv., 2.5 M in hexanes), THF (0.18 M, dry), -78 °C, 1 h, then methyl chloroformate (6 equiv.), -78 °C-rt, 1 h; h) 36% HCl (60 equiv.), THF (0.18 M), 0 °C-rt, 4 h.

(Teknokroma) capillary column (5% diphenyl-95% dimethylpolysiloxane, 10 m*0.1 nm*0.1 μm).

Synthesis of compounds 2a-o via Au NPs/TiO₂-catalysed cyclisation/reduction sequence

The corresponding aldehyde **1a-o** (0.5 mmol, 1 equiv.), 1% Au NPs/TiO₂ (245.7 mg, 2.5 mol%) and Hantzsch ester (151.9 mg, 0.6 mmol, 1.2 equiv.) was diluted in anhydrous toluene (2 mL, 0.25 M) under N₂ (Fig. 1a). This prepared heterogeneous reaction mixture was placed into preheated oil bath (80 °C) and stirred until the aldehyde **1a-o** was fully consumed—usually 2 h (reaction was followed by TLC and GC-MS as well). Once reaction was completed, the heterogeneous mixture was cooled to room temperature (Fig. 1b), filtered over short pad of SiO₂ by using of EtOAc (20 mL) as eluent (Fig. 1c). (EtOAc was selected as a solvent, to be sure, that all formed products will be collected). Solvent was then evaporated under reduced pressure and crude was analysed by ¹H NMR. The crude reaction mixture was then purified by SiO₂ column chromatography (eluent is specified for each compound).

Synthesis of compounds 3a-m via Au NPs/TiO₂-catalysed cyclisation/hydroalkoxylation sequence

The corresponding aldehyde **1a-m** (0.5 mmol, 1 equiv.), 1% Au NPs/TiO₂ (245.7 mg, 2.5 mol%) was diluted in anhydrous MeOH or MeOH/DMF 1:1 (2 mL, 0.25 M) under N₂ (Fig. 2a). This prepared heterogeneous reaction mixture was placed into preheated oil bath (70 °C) and stirred until the aldehyde **1a-m** was fully consumed—usually 2 h (reaction was followed by TLC and GC-MS as well). Once the reaction was completed, the heterogeneous mixture was cooled to room temperature (Fig. 2b), filtered over short pad of SiO₂ by using of EtOAc (20 mL) as eluent (Fig. 2c). Crude was then diluted with toluene (3 mL) and evaporated (procedure was repeated 4x to remove all traces of DMF, when applicable). Solvent was then evaporated under reduced pressure and product **3a-m** was isolated and fully characterised, with no necessity of further purification.

General procedure in flow conditions

The flow reactor set-up is shown in S.I. The set-up consists of a pump (Vapourtec R4 unit), an automated two-inlet valve (part of the Vapourtec R2C+ unit) allowed for rapid switching from pure solvent to the solution containing the dissolved reagent and a glass heated reactor (charged with Au NPs/TiO₂, 5 g). The reactor volume was determined by measuring the mass difference between reactor containing only catalyst and after filling with MeOH giving the volume of the reactor 5 mL. A back-pressure regulator device (Vapourtec, 8 bars) was installed to control the internal pressure of the system. PTFE tubing kit was selected for its thermal resistance, its flexibility and its high chemical resistance. The temperature in the reactor during the reaction is estimated to 70 °C based on temperature measurements taken between the reactor and the glass assy. Before the reaction the flow device was flushed with MeOH and the temperature was adjusted to 70 °C. Once a constant temperature of the solvent (flow rate 1.5 mL/min) was reached, a solution of aldehyde **1a** (9.7 mmol, 2 g) dissolved in anhydrous MeOH (0.1 M, 97 mL) was pumped through the system. The collection was performed during the steady state and the mixture analysed via TLC and GC/MS detector. Solvent was then evaporated under reduced pressure and product **3a** was isolated and fully characterised, with no necessity for further purification.

Data availability

The data that support the findings of this study are available from the corresponding author upon reasonable request.

Received: 17 June 2024; Accepted: 21 October 2024;

Published online: 30 October 2024

References

- Haruta, M., Kobayashi, T., Sano, H. & Yamada, N. Novel gold catalysts for the oxidation of carbon monoxide at a temperature far below 0 °C. *Chem. Lett.* **16**, 405–408 (1987).
- Nkosi, B., Coville, N. J. & Hutchings, G. J. Reactivation of a supported gold catalyst for acetylene hydrochlorination. *J. Chem. Soc. Chem. Commun.* 71–72 (1988).
- Hutchings, G. J. & Joffe, R. A novel process for the co-synthesis of vinyl chloride monomer and sodium carbonate using a gold catalyst. *Appl. Catal.* **20**, 215–218 (1986).
- Toste, F. D. & Michelet, V. *Gold Catalysis: an Homogeneous Approach*. pp. 546 (Imperial College Press, 2014).
- Rappoport, Z., Liebman, J. F., Marek, I. *The Chemistry of Organogold Compounds* (John Wiley & Sons, Inc., 2014).
- Slaughter, L. M. *Homogeneous Gold Catalysis* (Springer, 2015).
- Hashmi, A. S. K. & Hutchings, G. J. Gold catalysis. *Angew. Chem. Int. Ed.* **45**, 7896–7936 (2006).
- Pflästerer, D. & Hashmi, A. S. K. Gold catalysis in total synthesis—recent achievements. *Chem. Soc. Rev.* **45**, 1331–1367 (2016).
- Hashmi, A. S. K. Introduction: gold chemistry. *Chem. Rev.* **121**, 8309–8310 (2021).
- Carrettin, S., Blanco, M. C., Corma, A. & Hashmi, A. S. K. Heterogeneous gold-catalysed synthesis of phenols. *Adv. Synth. Catal.* **348**, 1283–1288 (2006).
- Abad, A., Corma, A. & García, H. Bridging the gap between homogeneous and heterogeneous gold catalysis: supported gold nanoparticles as heterogeneous catalysts for the benzannulation reaction. *Top. Catal.* **44**, 237–243 (2007).
- González-Arellano, C. et al. Catalysis by gold(I) and gold(III): a parallelism between homo- and heterogeneous catalysts for copper-free sonogashira cross-coupling reactions. *Angew. Chem. Int. Ed.* **46**, 1536–1538 (2007).
- Stratakis, M. & Garcia, H. Catalysis by supported gold nanoparticles: beyond aerobic oxidative processes. *Chem. Rev.* **112**, 4469–4506 (2012).
- Porta, R., Benaglia, M. & Puglisi, A. Flow chemistry: recent developments in the synthesis of pharmaceutical products. *Org. Process. Res. Dev.* **20**, 2–25 (2016).
- Mori, T. & Hegmann, T. Determining the composition of gold nanoparticles: a compilation of shapes, sizes, and calculations using geometric considerations. *J. Nanopart. Res.* **18**, 295 (2016).
- Zhou, X., Xu, W., Liu, G., Panda, D. & Chen, P. Size-dependent catalytic activity and dynamics of gold nanoparticles at the single-molecule level. *J. Am. Chem. Soc.* **132**, 138–146 (2010).
- Boronat, M., Leyva-Pérez, A. & Corma, A. Theoretical and experimental insights into the origin of the catalytic activity of subnanometric gold clusters: attempts to predict reactivity with clusters and nanoparticles of gold. *Acc. Chem. Res.* **47**, 834–844 (2014).
- Ishida, T., Taketoshi, A. & Haruta, M. in *Nanoparticles in Catalysis* (ed Shū Kobayashi) 1–48 (Springer International Publishing, 2020).
- Farokhpour, H., Abedi, S. & Jouypazadeh, H. Directional affinity of a spherical gold nanoparticle for the adsorption of DNA bases. *Colloids Surf. B Biointerfaces* **173**, 493–503 (2019).
- Notar Francesco, I., Fontaine-Vive, F. & Antonietti, S. Synergies in the catalytic activity of bimetallic nanoparticles and design of new synthetic methods for the preparation of fine chemicals. *ChemCatChem* **6**, 2784–2791 (2014).
- Chen, J., Fang, W., Zhang, Q., Deng, W. & Wang, Y. A comparative study of size effects in the Au-catalyzed oxidative and non-oxidative dehydrogenation of benzyl alcohol. *Chem. Asian J.* **9**, 2187–2196 (2014).
- Niu, K. et al. Mechanistic investigations of the Au catalysed C–H bond activations in on-surface synthesis. *Phys. Chem. Chem. Phys.* **20**, 15901–15906 (2018).
- Ishida, T., Murayama, T., Taketoshi, A. & Haruta, M. Importance of size and contact structure of gold nanoparticles for the genesis of unique catalytic processes. *Chem. Rev.* **120**, 464–525 (2020).

24. Oliver-Meseguer, J., Cabrero-Antonino, J. R., Domínguez, I., Leyva-Pérez, A. & Corma, A. Small gold clusters formed in solution give reaction turnover numbers of 10^7 at room temperature. *Science* **338**, 1452–1455 (2012).
25. Raptis, C., Garcia, H. & Stratakis, M. Selective isomerization of epoxides to allylic alcohols catalyzed by TiO₂-supported gold nanoparticles. *Angew. Chem. Int. Ed.* **48**, 3133–3136 (2009).
26. Efe, C., Lykakis, I. N. & Stratakis, M. Gold nanoparticles supported on TiO₂ catalyse the cycloisomerisation/oxidative dimerisation of aryl propargyl ethers. *Chem. Commun.* **47**, 803–805 (2011).
27. Gryparis, C., Efe, C., Raptis, C., Lykakis, I. N. & Stratakis, M. Cyclization of 1,6-enynes catalyzed by gold nanoparticles supported on TiO₂: significant changes in selectivity and mechanism, as compared to homogeneous Au-catalysis. *Org. Lett.* **14**, 2956–2959 (2012).
28. Nasrallah, H. O. et al. Nanocatalysts for high selectivity enyne cyclization: oxidative surface reorganization of gold sub-2-nm nanoparticle networks. *JACS Au* **1**, 187–200 (2021).
29. Laher, R., Marin, C. & Michelet, V. When gold meets perfumes: synthesis of olfactive compounds via gold-catalyzed cycloisomerization reactions. *Org. Lett.* **22**, 4058–4062 (2020).
30. Davenel, V. et al. Gold-catalyzed cycloisomerization of 1,6-cyclohexenylalkyne: an efficient entry to bicyclo[3.2.1]oct-2-ene and bicyclo[3.3.1]nonadiene. *J. Org. Chem.* **85**, 12657–12669 (2020).
31. Tang, Y. et al. An original L-shape, tunable N-heterocyclic carbene platform for efficient gold(I) catalysis. *Angew. Chem. Int. Ed.* **58**, 7977–7981 (2019).
32. Chen, X., Martini, S. & Michelet, V. A mild and regioselective synthesis of α -fluoroketones via gold and selectfluor partnership. *Adv. Synth. Catal.* **361**, 3612–3618 (2019).
33. Giorgi, P. D., Elizarov, N. & Antoniotti, S. Selective oxidation of activated alcohols by supported gold nanoparticles under an atmospheric pressure of O₂: batch and continuous flow studies. *ChemCatChem* **9**, 1830–1836 (2017).
34. Giorgi, P. D., Miedziak, P. J., Edwards, J. K., Hutchings, G. J. & Antoniotti, S. Bimetallic multistep reactions en route to the one-pot total synthesis of complex molecules: easy access to chromene and 1,2-dihydroquinoline derivatives from simple substrates. *ChemCatChem* **9**, 70–75 (2017).
35. Giorgi, P. D., Liautard, V., Pucheault, M. & Antoniotti, S. Biomimetic cannabinoid synthesis revisited: batch and flow all-catalytic synthesis of (\pm)-*ortho*-tetrahydrocannabinols and analogues from natural feedstocks. *Eur. J. Org. Chem.* **2018**, 1307–1311 (2018).
36. Notar Francesco, I. et al. Novel radical tandem 1,6-enynes thioacylation/cyclisation: Au-Pd nanoparticles catalysis versus thermal activation as a function of the substrate specificity. *Tetrahedron* **70**, 9635–9643 (2014).
37. Tomás-Mendivil, E., Starck, J., Ortuno, J.-C. & Michelet, V. Synthesis of functionalized 1H-isochromene derivatives via a Au-catalyzed domino cycloisomerization/reduction approach. *Org. Lett.* **17**, 6126–6129 (2015).
38. Nardangeli, N., Thomson, J., Topolovčan, N. & Hudlický, T. Total synthesis of methyl 1,5,8-trimethoxy-1h-isochromene-3-carboxylate and its derivatives via palladium-catalyzed annulation of 2-alkynylbenzaldehydes. *Synthesis* **53**, 4110–4116 (2021).
39. Tomás-Mendivil, E., Heinrich, C. F., Ortuno, J.-C., Starck, J. & Michelet, V. Gold-catalyzed access to 1H-isochromenes: reaction development and mechanistic insight. *ACS Catal.* **7**, 380–387 (2017).
40. Godet, T., Vaxelaire, C., Michel, C., Millet, A. & Belmont, P. Silver versus gold catalysis in tandem reactions of carbonyl functions onto alkynes: a versatile access to furoquinoline and pyranoquinoline cores. *Chem. Eur. J.* **13**, 5632–5641 (2007).
41. Wu, A., Qian, H., Zhao, W. & Sun, J. Benzannulation of isobenzopyryliums with electron-rich alkynes: a modular access to β -functionalized naphthalenes. *Chem. Sci.* **11**, 7957–7962 (2020).
42. Liu, S. et al. Mild intermolecular synthesis of a cyclopropane-containing tricyclic skeleton: unusual reactivity of isobenzopyryliums. *Angew. Chem. Int. Ed.* **60**, 21272–21276 (2021).
43. Attardo, G. et al. Antineoplastic heteronaphthoquinones (IAF Biochem Int [CA]), WO9512588 (1995).

Acknowledgements

This work was supported by Université Côte d'Azur, CNRS and by the French government through the France 2030 investment plan managed by the National Research Agency (ANR), as part of the Initiative of Excellence Université Côte d'Azur under reference number ANR-15-IDEX-01. We thank Thomas Davies from Translational Research Hub, Cardiff University (UK) for STEM analysis. We are grateful to the Université Côte d'Azur Office of International Scientific Visibility for English language editing of the manuscript.

Author contributions

K.P.: Data curation; formal analysis; investigation; methodology; validation; visualisation; writing—original draft; conceptualisation. V.M.: Data curation; formal analysis; methodology. S.A.: Data curation; formal analysis; methodology; validation; writing—original draft; writing—review & editing; conceptualisation; funding acquisition; project administration; resources; supervision.

Competing interests

The authors declare no competing interests.

Additional information

Supplementary information STEM analysis of Au NPs on TiO₂. Screening of conditions for the cyclisation/reduction sequence. Preparation of starting materials. Optimisation studies for both reactions. Negative control experiments and ICP-OES titration of soluble gold species. Detailed procedures and data for the synthesis of **2a-o** and **3a-o** both in batch and flow conditions, as well as **4a-6a** and the total synthesis of **10**. The online version contains supplementary material available at <https://doi.org/10.1038/s42004-024-01336-7>.

Correspondence and requests for materials should be addressed to Sylvain Antoniotti.

Peer review information *Communications Chemistry* thanks the anonymous reviewers for their contribution to the peer review of this work.

Reprints and permissions information is available at <http://www.nature.com/reprints>

Publisher's note Springer Nature remains neutral with regard to jurisdictional claims in published maps and institutional affiliations.

Open Access This article is licensed under a Creative Commons Attribution-NonCommercial-NoDerivatives 4.0 International License, which permits any non-commercial use, sharing, distribution and reproduction in any medium or format, as long as you give appropriate credit to the original author(s) and the source, provide a link to the Creative Commons licence, and indicate if you modified the licensed material. You do not have permission under this licence to share adapted material derived from this article or parts of it. The images or other third party material in this article are included in the article's Creative Commons licence, unless indicated otherwise in a credit line to the material. If material is not included in the article's Creative Commons licence and your intended use is not permitted by statutory regulation or exceeds the permitted use, you will need to obtain permission directly from the copyright holder. To view a copy of this licence, visit <http://creativecommons.org/licenses/by-nc/4.0/>.

© The Author(s) 2024